Available online at www.sciencedirect.com
SCIENCE DIRECT®

Journal of the European Ceramic Society 24 (2004) 1961–1967

www.elsevier.com/locate/jeurceramsoc

Macroporous and nanosized ceramic films prepared by modified sol-gel method with PMMA microsphere templates

Kazuhiro Sasahara, Takeo Hyodo, Yasuhiro Shimizu, Makoto Egashira*

Department of Materials Science and Engineering, Nagasaki University, 1-14 Bunkyo-machi, Nagasaki 852-8521, Japan

Abstract

Macroporous ceramic thick films consisting of nanosized particles have been fabricated successfully by a modified sol-gel method employing polymethylmethacrylate (PMMA) microspheres as a template. PMMA microspheres with a uniform particle size (mean diameter: 870 nm) were first deposited on an oxidized silicon substrate. Precursor solutions of $Ti(i\text{-}C_3H_7O)_4$ in isopropyl alcohol, $SnCl_2 2H_2O$ in dehydrated ethanol and $MgCl_2 6H_2O$ in a mixture of ethanol and ultra pure water permeated into the openings of the template layer in vacuo, and then was air-dried at room temperature. The composite layers were subjected to heat treatment at 500–600 °C in air in order to remove the core PMMA templates by thermal decomposition and then to oxidize the precursor frameworks. In the case of a macroporous SnO_2 thick film, this heat treatment resulted in formation of a self-standing network of interconnected hollow SnO_2 microspheres whose shell walls consisted of nanosized oxide particles about 40 nm in diameter.

Keywords: Hollow SnO_2 microspheres; Macroporous thick film; PMMA; Sol-gel processes; Template

1. Introduction

Recently, macroporous materials with three-dimensionally (3-D) ordered arrays of pores with diameters from tens to hundreds of nanometers have commanded interest in a wide range of application (both structural and functional): e.g., as photonic crystals for optical communication devices, supports for catalytic agents and electronic industry materials for sensor devices and electrodes, because of a full photonic band-gap effect, high specific surface area and low thermal conductivity [1–7]. The most common method used for assembling highly ordered porous structure is a colloidal crystal templating method with a well-ordered packed structure of silica or polystyrene (PS) microspheres [4–14]. Typical examples are as follows. Zakhidov et al. have fabricated a variety of macroporous carbons that are 3-D periodic on the scale of optical wavelengths [11]. In their study, a silica opal was used as a template, whose openings were filled with carbon or a material that converts to carbon. 3-D ordered macroporous metal oxides including many transition metal oxides and alkaline earth metal oxides have been prepared by Yan et al. with a templated precipitation/chemical conversion method employing a 3-D ordered array of PS spheres, i.e. PS latex centrifugation, metal ion impregnation, oxalate precipitation, and subsequent conversion to macroporous metal oxides [13]. Wang et al. have controlled successfully pore morphology of 3-D ordered macroporous TiO_2 (e.g., wall thickness and open/closed pore structure of resulting macroporous materials) by using the PS spheres coated with polyelectrolyte multilayers as a template [14].

From the viewpoint of easy removal of templates without any fracture of 3-D ordered macroporous frameworks, i.e. easy thermal decomposition of polymeric templates, we believe that spherical polymethylmethacrylate (PMMA) is an alternative template [15,16], although spherical PS has been used widely as a polymeric template in the colloidal crystal templating method [12–14, 17].

The aim of the present study is to establish the most suitable fabrication conditions of macroporous oxide thick film consisting of nanosized particles by a modified sol-gel method employing PMMA microspheres as a template. The films fabricated were SnO_2, TiO_2 and

* Corresponding author: Tel.: +81-95-819-2642; fax: +81-95-819-2643.
E-mail address: egashira@net.nagasaki-u.ac.jp (M. Egashira).

0955-2219/$ - see front matter © 2003 Elsevier Ltd. All rights reserved.
doi:10.1016/S0955-2219(03)00518-1

MgO, the former two being the most important gas sensor materials.

2. Experimental

2.1. Fabrication of macroporous ceramic thick films

Non-crosslinked polymethylmethacylate (PMMA) microspheres with a nominal uniform particle size of 800 nm were purchased from Soken Co., Ltd (MP-1600) and were used as a template. Three grams of the PMMA microspheres was dispersed in 5.0 g ultra pure water (resistivity higher than 18.2 MΩcm) supplied by a three-stage Milli-Q (Millipore, EQ-5S) purification system. To the colloidal suspension was added 0.05 g ammonium polycarboxylic acid as a dispersing agent. To ensure dispersing of PMMA microspheres, the suspension was sonicated by an ultrasonic device for 30 min. Then, the suspension was dip-coated on an oxidized silicon wafer. The substrate dip-coated with the suspension was air-dried at room temperature. PMMA microspheres could self-assemble into a 3-D array by sedimentation during the drying process.

Oxide precursor solutions employed in the present study were as follows, unless otherwise noted: 5.0 ml $Ti(i\text{-}C_3H_7O)_4$ (99%, Rare Metallic Co., Ltd.) in 5.0 ml isopropyl alcohol (99.5%, Wako Chemical. Industries, Ltd.), 2.3 g (1.0 mol/l) $SnCl_2 2H_2O$ (97%, Kishida. Co., Ltd.) in 10 ml dehydrated ethanol (99.5 vol.%, Wako Chemical Industries), and 2.0 g (1.0 mol/l) $MgCl_2 6H_2O$ in a mixture of 5.0 ml ethanol and 5.0 ml ultra pure water. The combination of source materials and solvents was determined by referring to both the reactivity with water and the solubility of source materials in solvents.

The precursor solution was permeated into the openings of the 3-D array of PMMA microspheres in vacuo, and then was air-dried at room temperature. A 3-D framework of a source material could be formed during this drying process. Especially in the case of $Ti(i\text{-}C_3H_7O)_4$ formation of a tight framework could be expected by uts hydrolysis and polymerization with a help of water vapor contained in the ambient atmosphere. Thereafter, the composite layer of the 3-D array of PMMA and the 3-D framework of the source material was subjected to heat treatment in flowing air in order to remove the core PMMA microspheres by thermal decomposition and then to oxidize the source material to form a macroporous oxide framework: slow heating at a rate of 1 °C min^{-1} up to 250 °C, fast heating at 10 °C min^{-1} ip to 400 °C and 2 h holding for the PMMA decomposition, slow heating at 1 °C min^{-1} up to 500 (for MgO thick film) or 600 °C (TiO_2 and SnO_2 thick films) and 2 h holding at the temperature for the oxidation and sintering.

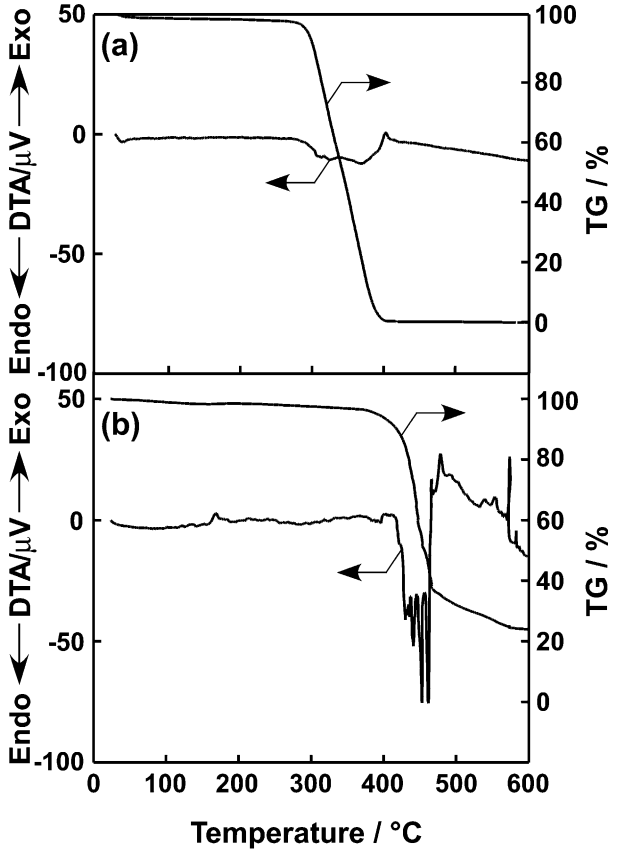

Fig. 1. TG–DTA curves for (a) PMMA microspheres and (b) PS latex measured at a heating rate of 10 °C min^{-1} in flowing air.

2.2. Characterization

Thermal decomposition behavior of PMMA microspheres was investigated by thermogravimetric and differential thermal analysis (TG-DTA, Shimadzu, DTG-50) up to 600 °C at a heating rate of 10 °C min^{-1} in flowing air. For comparative purpose, thermal decomposition behavior of polysthyrene (PS) latex microspheres with a mean particle size of 700 nm (JSR Corp., No. 0561) was also studied.

Crystal phase and crystallite size of the oxide thick films fabricated were characterized by X-ray diffraction (XRD, Rigaku, RINT-2200). Specific surface area was measured by BET method using a N_2 sorption isotherm (Micromeritics, TriStar 3000). Morphology and macroporous structure of the oxide thick films were observed by a scanning electron microscope (SEM, Hitachi, S-2250N) and a transmission electron microscope (TEM, Jeol, JEM2010-HT).

3. Results and discussion

3.1. Thermal decomposition behavior of PMMA microspheres

Thermal decomposition behavior of polymeric template materials is considered to be one of the important

factors to control morphology of macroporous ceramic thick films prepared by a colloidal crystal templating method. Fig. 1 compares TG–DTA curves between PMMA and PS latex. In the case of PMMA, gradual and slight weight loss (about 2.3% of the total weight loss) was observed up to 270 °C, and beyond that an abrupt decrease in weight was observed in a narrow temperature range of 300–380 °C, and then PMMA disappeared completely up to about 390 °C. The first slight weight loss may be ascribed to desorption of water. In accordance with the second abrupt weight loss, a broad endothermic peak appeared in a temperature range of 290–390 °C. In addition, a very small exothermic peak was observed around 400 °C. Thus, it is expected that PMMA is pyrolyzed directly to gaseous species without forming any molten states during its thermal decomposition. We believe such decomposition behavior is essential for maintaining the ordered 3-D macroporous frameworks during the removal process of templates. In contrast, PS latex exhibited an abrupt weight loss, but about 63% loss of total weight, in a higher temperature range (420–470 °C) than that for PMMA, and left behind a certain amount of, presumably, a carbonaceous residue (about 24% of total weight) even after firing up to 600 °C. In addition, appearance of several endothermic peaks in the temperature range of 420–470 °C and exothermic peaks above 470 °C implies very complex decomposition process including melting, vaporization and combustion of decomposed products. From the viewpoint of easy and complete removal of template materials without any fracture of 3-D ordered macroporous frameworks, therefore, we adopted PMMA microspheres with uniform particle size as a template material in the present study.

3.2. Pore morphology in macroporous ceramic thick films

Fig. 2(a) and (b) shows surface and cross-sectional views of a 3-D array of PMMA microspheres fabricated on an oxidized silicon substrate by dip coating. Particle size of PMMA microspheres was almost uniform, while some large particles were observed. Mean particle size was measured to be 870 nm by SEM observation, which was slightly bigger than the nominal value. Hexagonal close-packing of PMMA microspheres was obvious in some parts of the surface of the PMMA layer, but some small voids also appeared. The layer of PMMA microspheres showed a good adhesive property sufficient for the subsequent permeation of the precursor solutions. No significant cracking of the PMMA layer was observed on the surface as well as in the layer after the permeation of the $SnCl_2 2H_2O$ precursor solution, as shown in Fig. 2(c) and (d), although small cracking was obvious in low magnification SEM photographs (not shown here). It is also obvious that PMMA microspheres are connected tightly to each other with the dried precursor material, i.e. the narrow openings along the surface of PMMA microspheres are filled with the dried precursor material, and that closer hexagonal packing appears. Similar morphology was observed for composite layers

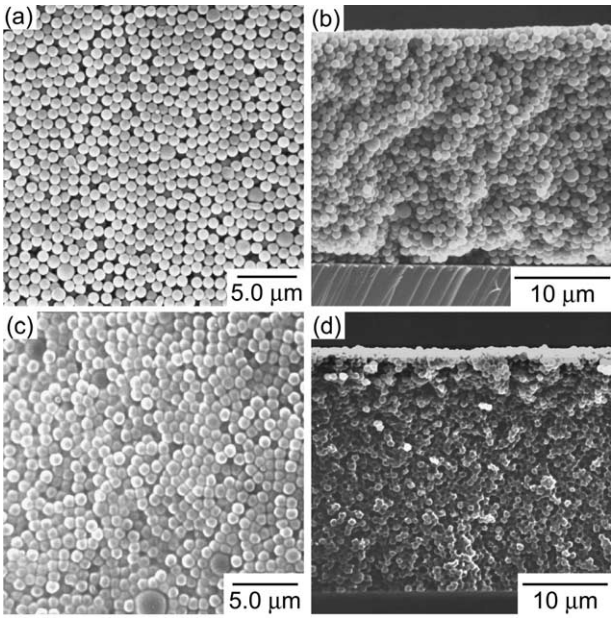

Fig. 2. SEM photographs of a self-assembled 3-D array of PMMA microspheres deposited on an oxidized silicon substrate (a, b) before and (c, d) after permeation of $SnCl_2 2H_2O$ precursor solution (2.3 g (1.0 mol/l) $SnCl_2 2H_2O$ dissolved in 10 ml dehydrated ethanol). Surface views: (a) and (c), cross-sectional views: (b) and (d).

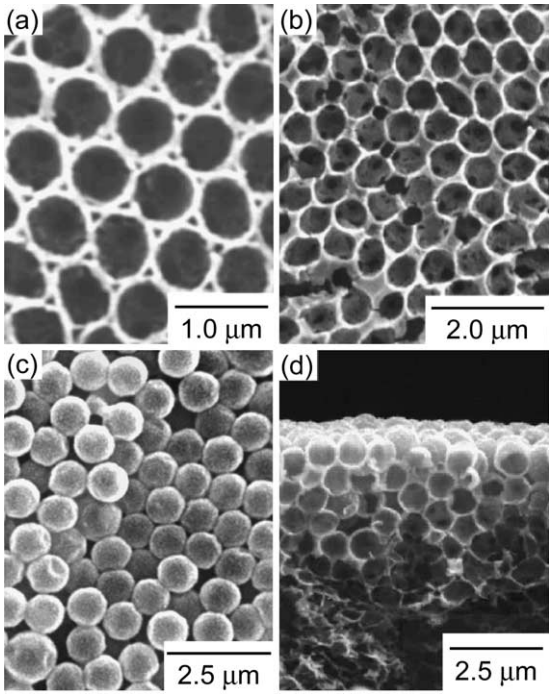

Fig. 3. SEM photographs of macroporous ceramic thick films fabricated on an oxidized silicon substrate. Surface films (a) TiO_2 (b) MgO (c) SnO_2 and cross-sectional view: (d) SnO_2 sectional view.

fabricated with other precursor solutions, while SEM photographs are not shown here.

XRD analysis revealed the formation of respective metal oxide layers, i.e. TiO_2, MgO and SnO_2 after removal of the templates. The surface of the macroporous oxide thick films fabricated on an oxidized silicon substrate was compared in Fig. 3. 3-D ordered self-standing frameworks were observed for every film, but the appearance of surface pore morphology was different from one to another depending on the kind of precursor materials. Among the films fabricated, the TiO_2 film showed the most ordered honeycomb pore structure, as shown in Fig. 3(a). Besides spherical macropores of about 630 nm in diameter, which reflects the void formed by the removal of PMMA microspheres, small pores appears at the boundaries of three spherical macropores. Thus, a shrinkage of 27% was calculated for the micropores, based on the original size of PMMA microspheres, in the case of the TiO_2 film. Each pore is partitioned with a TiO_2 framework (about 7.0 μm thick) with a crystallite size of 25.9 nm. The surface area of the 3-D ordered macroporous TiO_2 thick film was 48.8 $m^2\ g^{-1}$ (see Table 1). However, adhesion of the film to the oxidised silicon substrate was weak. The adhesion properties of the film could not be improved under the present fabrication conditions, even when an ITO glass was employed as an alternative substrate.

The MgO film also exhibited a macroporous framework, as shown in Fig. 3(b), but, the pores were not spherical but distorted after calcination. Mean size of distorted pores was 550 nm and, therefore, the pore shrinkages was 36%. Such a large shrinkage is considered to arise from the lowest metal concentration among the precursor solutions employed and poor wettability between the precursor solution and the PMMA microspheres. Weak mechanical strength of the dried precursor material or the oxide shell wall might facilitate the distortion of the pores during removal of PMMA. However, the MgO film exhibited good adhesive properties against the oxidized silicon substrate. A cross-sectional view also showed the distorted macropore structure of the MgO film. In addition, the MgO film was characterized with a very small surface area of 5.4 m^2g^{-1}, whereas the crystallite size was 8.4 nm, as summarized in Table 1, suggesting a rapid grain growth during calcination.

In contrast, well interconnected microspheres appeared after calcination in the case of SnO_2 thick film, as shown in Fig. 3(c). From the cross-sectional view of the film shown in Fig. 3(d), it is obvious that the microspheres are hollow without any large holes on their surface. Formation of such hollow SnO_2 microspheres is due to unique decomposition behavior of PMMA, i.e. presumably rapid evolution of decomposed gaseous components from PMMA through a still porous dried precursor material in the shell structure, but with sufficient strength, and no fusion of PMMA during the decomposition. The mean size of the hollow SnO_2 microspheres was 1.15 μm, while the mean inner pore diameter was about 720 nm. Therefore, the pore shrinkage was about 16%. From the high magnification SEM and TEM photographs shown in Fig. 4(a) and (b), it is apparent that the hollow microspheres connected to each other have a relatively rough surface, indicating that the shell walls are rather porous. The crystallite size of the hollow SnO_2 microspheres was calculated to be 8.7 nm based on the XRD data and this value was confirmed by the hEM observation in Fig. 4(b). The surface area of the macroporous SnO_2 thick film was 41.8 m^2g^{-1} (see Table 1), The SnO_2 film also exhibited good adhesive properties against the oxidized silicon substrate. However, some distorted hollow microspheres were observed, especially in the innermost region of the thick film, as shown in Fig. 3(d), probably due to the weak strength of the shell wall associated with low metal concentration in the precursor solution and also the gravitation of overlying microspheres themselves.

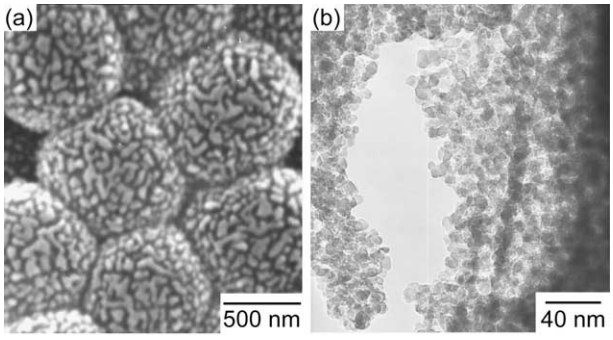

Fig. 4. (a) High magnification SEM photograph of hollow SnO_2 microspheres and (b) TEM photograph of the shell part of a hollow SnO_2 microsphere.

Table 1
Microstructure and surface area for macroporous ceramic film

Oxide layer	Crystallite size[a] (nm)	BRT surface area (m^2/g)	Macropore diameter (nm)	Shrinkage of pores (%)
TiO_2	25.9	48.8	630	27
MgO	–	5.4	550	36
SnO_2	8.7	41.8	720	16

[a] Crystallite size was calculated by Scherrer's equation based on the XRD data.

3.3. Effect of concentration of precursor solution on resulting SnO_2 macroporous structure

We believe that the pore structure of macroporous films (diameter and shape of macropores, strength of shell wall, end etc.) was affected by several factors; e.g. size of template particles, the kind and concentration of precursor solutions, heat treatment conditions. Especially, the concentration of precursor solutions may be important for preventing collapse of the inorganic shell walls of the macropores during decomposition and gasification of PMMA templates. Thus, macroporous SnO_2 films were fabricated with different concentrations of the precursor solutions. Fig. 5 shows SEM photographs of the macroporous SnO_2 thick films fabricated with the lower (1.13 g (0.5 mol/l)) and higher (4.51 g (2.0 mol/l)) concentration of $SnCl_2 2H_2O$ in 10 ml dehydrated ethanol. When the concentration was low, a SnO_2 framework with hemispherical fringes and distorted pores appeared on the surface of the layer and no closed SnO_2 microspheres were found [see Fig. 5(a)]. This surface morphology was similar to that observed for the MgO film shown in Fig. 3(b). In addition, a large number of distorted hollow microspheres were observed in its cross-sectional view, as shown in Fig. 5(b). The low concentration of the precursor solution and in turn weak strength of the resulting SnO_2 shell wall is undoubtedly responsible for such morphology of the mesoporous thick film. On the other hand, almost all the SnO_2 microspheres were closed in the case of the high concentration of $SnCl_2 2H_2O$, although some had cracks on their surface, as shown in Fig. 5(c). Closed SnO_2 microspheres also appeared on the cross-section of the film, as shown in Fig. 5(d), presenting a striking contrast to the cases of lower concentration of $SnCl_2 2H_2O$ [compare with Figs. 3(d) and 5(b)], while the SnO_2 microspheres were again confirmed to be hollow (not shown here). In this case, the layer of SnO_2 microspheres is obviously fractured at the neck boundaries of the hollow microspheres, indicating that the shell wall of each microsphere is relatively strong. Anyway, it is confirmed that the structure of macroporous SnO_2 thick films can be modified by controlling the concentration of the precursor solution.

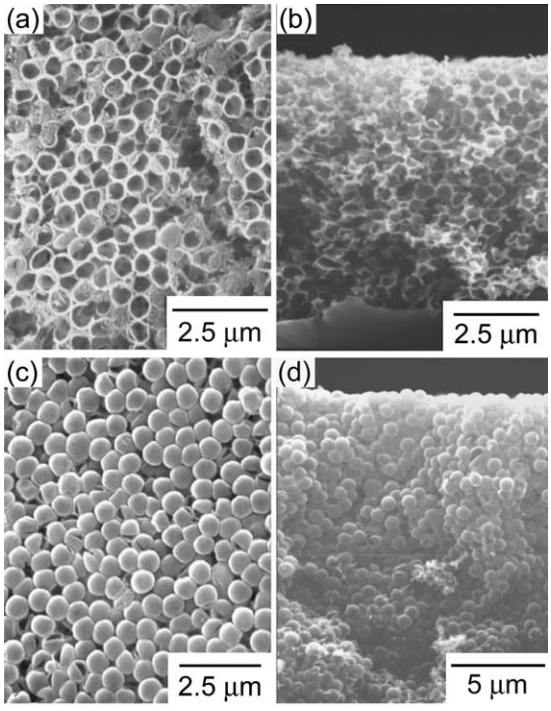

Fig. 5. SEM photographs of SnO_2 thick films fabricated from the $SnCl_2 2H_2O$ precursor solution of different concentrations. The amount of $SnCl_2 2H_2O$ dissolved in 10 ml ethanol is 1.13 g (0.5 mol/l) for (a) and (b) and 4.51 g (2.0 mol/l) for (c) and (d). Surface views: (a) and (c), cross-sectional views: (b) and (d).

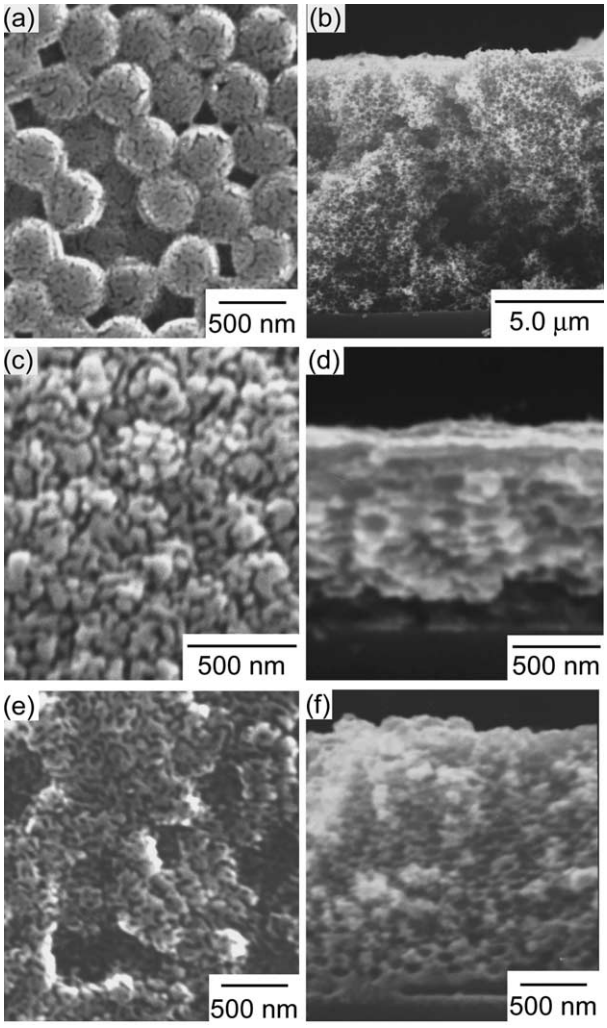

Fig. 6. SEM photographs of SnO_2 thick films fabricated with different size of PMMA microspheres (Precursor solution: 2.3 g (1.0 mol/l) $SnCl_2 2H_2O$ in 10 ml dehydrated ethanol). Mean particle size of PMMA employed is 400 for (a) and (b), 250 for (c) and (d), and 150 nm for (e) and (f). Surface views: (a), (c) and (e), cross-sectional views: (b), (d) and (f).

3.4. Effect of particle size of PMMA on resulting SnO_2 macroporous structure

Particle size of PMMA microspheres as a template may also be an important factor determining the framework of the resulting macroporous SnO_2. Thus, effect of particle size of PMMA templates has been examined by employing the same concentration of $SnCl_2 2H_2O$ precursor solution (2.3 g (1.0 mol/l) $SnCl_2 2H_2O$ in 10 ml dehydrated ethanol). PMMA microspheres employed additionally were also purchased from Soken. Co., Ltd and were 400 nm (MP-1000), 250 nm (MP-1450) and 150 nm (MP-1451) in mean diameter. When 400 nm PMMA microspheres were used, a layer of interconnected hollow SnO_2 microspheres could be fabricated, as shown in Fig. 6(a) and (b), though a hole or crack was found on the surface of some microspheres and a large number of distorted hollow microspheres appeared in its cross-sectional view. In the cases of PMMA microspheres less than 250 nm in diameter, formation of ordered spherical SnO_2 microspheres was rarely found in the surface of the layers (see Figs. 6(c) (e)), although distorted macropore structure was visible in some parts of the layers in the cross-sectional views (see Fig. 6(d) and (f)). Thus, it is found that the use of bigger PMMA microspheres tends to facilitate formation of a more ordered macroporous structure, although the reason for this phenomenon is not clear at present.

From the results described above, it has been revealed that a very unique macroporous thick film of ordered hollow SnO_2 microspheres could be fabricated by employing PMMA microspheres bigger than 400 nm in diameter under the present experimental conditions. Such a macroporous SnO_2 thick film could also be successfully fabricated on an alumina substrate equipped with interdigitated Pt electrodes, though the results are not shown here. Thus, application of such a SnO_2 thick film to a sensor material is of great interest, and is now under investigation.

4. Conclusion

Macroporous ceramic thick films consisting of nanosized oxide particles have been fabricated successfully by a modified sol-gel method employing polymethylmethacrylate (PMMA) microspheres as a template. PMMA microspheres are considered to be a suitable template from the thermal decomposition behavior. In the case of SnO_2 films, the resulting macropores after removal of the PMMA microspheres were in a self-standing framework of interconnected hollow microspheres whose porous shell walls consisted of nanosized oxide particles less than about 40 nm in diameter, when PMMA microspheres bigger than 400 nm in diameter were employed. In this method, macroporous structure, e.g. pore diameter, shape (opened or closed) and framework thickness, could be controlled by varying the particle size of PMMA microspheres and the concentration of precursor solutions.

Acknowledgements

The present work was partly supported by Grant-in-Aid for Scientific Research (B) (No. 13555175) from Japan Society for the Promotion of Science and Industrial Technology Research Grant Program in '02 (No. 0725001) from New Energy and Industrial Technology Development Organization (NEDO) of Japan.

References

1. Yablonovitch, E., Inhibited spontaneous emission in solid-state physics and electronics. *Phys. Rev. Leit.*, 1986, **58**, 2059–2062.
2. Joannopoulos, J. D., Villeneuve, P. R. and Fan, S., Photonic crystals: putting a new twist on light. *Nature*, 1997, **386**, 143–149.
3. Lin, Y., Fleming, J. G., Hetherington, D. L., Smith, B. K., Biswas, R., Ho, K. M., Sigalas, M. M., Zubrzycki, W., Kurtz, S. R. and Bur, J., A three-dimensional photonic crystal operating at infrared wavelengths. *Nature*, 1998, **394**, 251–253.
4. Noda, S., Tomoda, K., Yamamoto, N. and Chutinan, A., Full three-dimensional photonic bandgap crystals at near-infrared wavelengths. *Science*, 2000, **289**, 604–606.
5. Wijnhoven, J. E. G. J. and Vos, W. L., Preparation of photonic crystals made of air sphere in titania. *Science*, 1998, **281**, 802–804.
6. Schroden, R. C., Al-Daous, M. and Stein, A., Self-modification of spontaneous emission by inverse opal silica photonic crystals. *Chem. Mater.*, 2001, **13**, 2945–2950.
7. Stein, A., Sphere templating methods for periodic porous solids. *Microporous and Mesoporous Materials*, 2001, **44-45**, 227–239.
8. Kawashita, T., Ohtera, Y. and Sato, T., Photonic crystals-functional optical materials. *Bull. Ceram. Soc. Jpn.*, 2002, **37**, 361–367.
9. Imhof, A. and Pine, D. I., Ordered macroporous materials by emulsion templating. *Nature*, 1997, **389**, 948–951.
10. Holland, B. T., Blanford, C. F. and Stein, A., Synthesis of macroporous minerals with highly ordered three-dimensional arrays of spherical voids. *Science*, 1998, **281**, 538–540.
11. Zakhidov, A. A., Baughman, R. H., Iqbal, Z., Cui, C., Khayrullin, I., Dantas, S. O., Marti, V. D. and Ralchenko, V. G., Carbon structures with three-dimensional periodicity at optical wavelengths. *Science*, 1998, **282**, 897–901.
12. Holland, B. T., Blanford, C. F., Do, T. and Stein, A., Synthesis of highly ordered, three-dimensional, macroporous structures of amorphous or crystalline inorganic oxides, phosphates, and hybrid composites. *Chem. Mater.*, 1999, **11**, 795–805.
13. Yan, H., Blanford, C. F., Holland, B. T., Smyrl, W. H. and Stein, A., General synthesis of periodic macroporous solids by templated salt precipitation and chemical conversion. *Chem. Mater.*, 2000, **12**, 1134–1141.
14. Wang, D., Caruso, R. A. and Caruso, F., Synthesis of macroporous titania and inorganic composite materials from coated colloidal spheres—a novel route to tune pore morphology. *Chem. Mater.*, 2001, **13**, 364–371.
15. Kato, T., Ushijima, H., Katsumata, M., Hyodo, T., Shimizu, Y. and Egashira, M., Preparation of core/shell microspheres of polymethylmethacrylate/alumina by mechanofusion as a precursor of hollow alumina microspheres. *Molecular Crystals and Liquid Crystals*, 2002, **376**, 101–106.

16. Kato, T., Ushijima, H., Katsumata, M., Hyodo, T., Shimizu, Y. and Egashira, M., Fabrication of hollow alumina microspheres via core/shell structure of polymethylmetha-crylate/alumina prepared by mechanofusion. *J. Mater Sci*., 2002, **36**, 2317–2321.

17. Stein, A. and Schroden, R. C., Colloidal crystal templating of three-dimensionally ordered macroporous solids: materials for photonics and beyond. *Current Opinion in Solid State and Materials Science*, 2001, **5**, 553–564.